

Fuzzy Predictive Energy Management for Hybrid Energy Storage Systems of Pure Electric Vehicles using Markov Chain Model

Qiao Zhang^{1,*}, Lijia Wang¹, Gang Li¹ and Shaoyi Liao²

¹ School of Automobile and Traffic Engineering, Liaoning University of Technology, Jinzhou 121000, China

² Information systems Department, City University of Hong Kong, Hong Kong, 999077, China.

Corresponding author: Q. Zhang

*E-mail: zq_625@163.com

Received: 21 July 2020 / Accepted: 13 September 2020 / Published: 30 September 2020

This paper describes a fuzzy predictive energy management strategy for battery and supercapacitor hybrid energy storage systems of electric vehicles and validates it using a scaled down experimental test platform. The strategy consists of a power demand distributor for dealing with power flow between battery and supercapacitor and a power demand predictor for improving the control performance of the former. The power demand distributor is developed based on a combination of filtration strategy and fuzzy logic controller. The filtration strategy is used to prevent battery from providing high frequency power demand. The fuzzy logic controller is used to shave battery peak current and maintain the voltage level of supercapacitor. Considering the stochastic nature of actual traffic condition, the power demand predictor is developed using a Markov chain model. Different from prior research efforts that carry out Markov decisions using either weighted probability estimation or maximum probability estimation, this study implement a comparative study on the two probability estimation methods based on NEDC, NurembergR36 and SC03 driving cycles. Experimental results validated the superiority of the described control strategy.

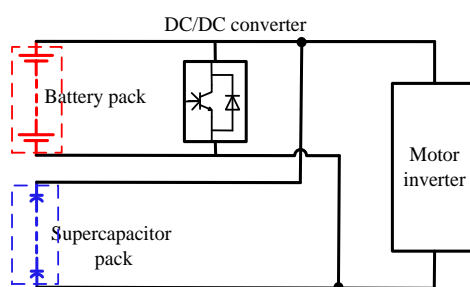
Keywords: Battery, supercapacitor, hybrid energy storage system, Markov decisions.

1. INTRODUCTION

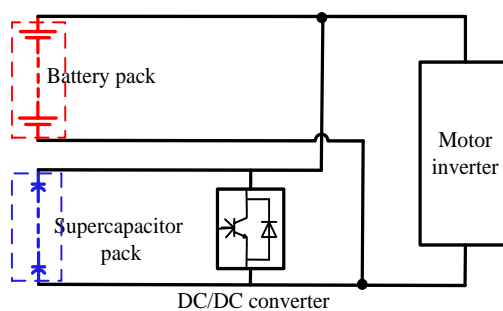
Along with petrol-driven automobile quantity increases as well as the air quality in cities and urban areas declines, the emission performance of cars has become a serious concern. In some automobile markets, such as China, United States and European Union, series of regulations have been issued in automotive sector to restrict emission of harmful gas, including CO, NO_x, HC and solid suspended particle[1]. These policies have heartened the development of electric vehicles, which have

been believed the most promising solution by automobile manufacturers[2]. However, the spread of electric vehicles has been slow, in part because of battery performance limitations. At present, lithium-ion batteries are most configured in electric vehicles for a continuous energy supply to satisfy the desired driving distance. In addition, spike power with large current demand often needs to be responded in time for vehicle performance and energy recovery during the process of vehicle acceleration and deceleration. Therefore, it requires batteries have not only high energy density and but also high power density at the same time for satisfying various driving demands of electric vehicles. However, owing to current technology limitation, it is still impossible to find the two natures in one battery[3,4].

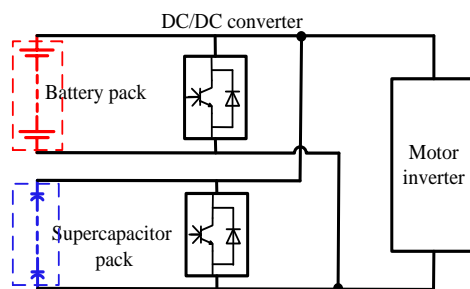
To break the battery performance dilemma, a hybrid energy storage system with battery pack as primary energy buffer and supercapacitor pack as primary power buffer, has been recommended in the literature. Compared with batteries, supercapacitors have higher power density but extremely low energy density. They are thus ideal partners combining with battery, compensating mutually flaws[5-10]. To form such a hybridized energy storage system, different kinds of topology structures have been proposed. Among these topology structures, the semi-active and fully active are most used[11-19], and three representative examples are shown in Figure 1. Generally, only one converter is employed in the semi-active topology structures for implementing power distribution task. The role of the DC/DC converter is to adjust current of a certain energy source with its voltage maintain. For the semi-active topology structure shown in Figure 1(a), the use of the supercapacitor can be obviously restrained when a stable load voltage needs to be maintained. Another kind of semi-active topology structure is illustrated in Figure 1(b). In this structure, since the supercapacitor can be actively controlled by the DC/DC converter, therefore the energy utilization efficiency can be obviously improved. The fully active topology structure with two DC/DC converters is given in Figure 1(c). Although this kind of structure can achieve best flexible control potential, it has the highest cost among all these structures.



(a) Semi-active topology structure with one degree of freedom: controllable battery.



(b) Semi-active topology structure with one degree of freedom: controllable supercapacitor.



(c) The fully active topology structure with two degrees of freedom: controllable battery and supercapacitor.

Figure 1. Three representative examples of the semi-active and fully active topology structures.

The performance of the mixed dual energy sources is heavily dependent upon the adopted energy management control strategy, which determines how much power demand would be delivered to battery and supercapacitor respectively. To improve the overall system efficiency and the battery durability, the development of highly efficient energy management strategies for hybrid energy storage systems has become a research hotspot in the field of hybrid electric vehicles. Some researchers have summarized the existing energy management strategies and classified them into two groups, which are optimization-based control strategies and rule-based control strategies, according to the described mathematical models when they are developed [8,20,21].

Optimization-based strategies aim at finding best solution to minimize the preset objective functions by employing some optimization algorithms, where common examples are dynamic programming [22], particle swarm optimization [23], genetic algorithm [24], DIRECT global optimization[25]. They are effective in seeking for ideal global results based on priori information of an entire driving cycle, but time-consuming. Therefore, they cannot be implemented online. On the contrary, their solutions are often used for parameter adjusting of some rule-based strategies. In order to improve the availability of optimization methods, some real-time optimization energy management strategies are proposed. In [26], the authors used equivalent consumption minimization strategy (ECMS) to online optimize power flow among the power systems. In the ECMS, the battery charge is converted

to the equivalent fuel coefficient, and the total fuel consumption (actual and equivalent) is minimized at each sampling interval. In [27], a model predictive controller (MPC) was developed for real-time power flow optimization during operation, considering physical constraint limitations of each power source in the system.

In contrast, rule-based methods are most designed through a series of preset rules which are inspired by heuristics and expertise experience. The development of the rules does not rely accurate mathematical model and priori knowledge of a driving cycle, therefore they have good real-time performance and robustness, and have been successfully employed in real hardware controllers, even though the solutions are not the most perfect. Determined rule, fuzzy logic and filtration strategies are three typical examples. In [28], the authors developed a multi-level power management strategy for such a compounded system. The determined rule-based strategies were designed for energy planning. Simulation showed the strategy could effectively reduce system losses and component sizing. In [29], a determined rule-based multi-mode energy management strategy was developed for switching working modes of battery and supercapacitor. Simulation and experimental results demonstrated that the proposed strategy could effectively reduce the energy losses of the DC/DC converter. In [30], the author used a determined rule-based strategy to control the charge and discharge of supercapacitor. Simulation results revealed that the control strategy allowed for a high utilization of supercapacitor for regenerative braking energy recovery. The determined rule strategy can realize good control performance by tuning rule parameters reasonably. Furthermore, in order to better accommodate the inherent time-varying and nonlinear characteristics of battery and supercapacitor hybrid energy system, fuzzy logic-based strategies are further put forwarded in [31-33]. For example, an adaptive fuzzy controller was built in [33]. In this strategy, the membership functions of the fuzzy controller are independently designed according to four different speed ranges of driving cycles. Experimental results demonstrated that the strategy had a good adaptation to variation of vehicle speed. Filtration-based strategy decomposes load power demand into different frequency components depending the characteristics of power sources. In [34], wavelet based filter power distribution strategy was introduced for a fuel cell system combined with battery and supercapacitor two sources. In this work, the load power was separated into high and low two frequency components using a three-layer Haar wavelet. The extracted low-frequency power demands were jointly assumed by the fuel cell stack and battery pack, while the high frequency part was distributed to the supercapacitor. Simulation and experimental results demonstrated the method could achieved satisfactory performance.

In summary, the rule-based strategies have good real-time capability, but fail to achieve optimal system performance. On the contrary, the ideal power sequences of each power source can be obtained by the optimization-based strategies, however they are not directly implementable because the computation process are time-consuming. For this, predictive energy management strategies, in which algorithms are performed at a short time window of future driving condition, are proposed by some researchers [35-37]. In general, the ahead knowledge of driving condition, including terrain, speed, distance and other data can be acquired by vehicular navigation system and radar sensors [36-38]. These telematic devices usually can supply high enough prediction accuracy, but their equipment cost is often very expensive. For this, low-cost mathematical algorithms, such as artificial neural networks and Markov chain models, are most used in predictive energy management strategies. The neural networks

have good learning and recognizing abilities, and therefore they are widely employed in the field of pattern recognition [39]. The learning vector quantization neural network was employed to develop a driving mode recognizer in [40]. For each driving mode, thermostat strategy was optimized by genetic algorithm. Simulation results showed that prediction-based multi-mode strategy could achieve better economic performance compared with the sole thermostat strategy under a composite profile which was based on a combination of three standard driving cycles. Considering the stochastic influences of traffic condition and driver operation, in [36], the Markov chain model, which assumed that the upcoming traffic and driver behaviors were independent of the past, was developed for power demand prediction. In this work, the predictive information was integrated into a fuzzy logic controller. Simulation and experimental results showed improved performance in peak current reduction and energy efficiency could be realized. In [41], a predictive energy management strategy based on a combination of Markov chain and Pontryagin's Minimum Principle was proposed for a fuel cell and supercapacitor hybrid system. Simulation results showed that the influence of speed variation on fuel cell hybrid system could be effectively reduced when Markov chain modular was added to the original strategy. In [42], a multi-mode energy management strategy based on driving pattern recognizer using Markov chain was proposed for fuel cell hybrid vehicles. In this study, three driving patterns are predefined according to speed-acceleration characteristics of driving cycles. Namely, each driving pattern was comprised of driving cycles that had similar Markov transition probability matrix. Simulation results showed that the hydrogen consumption could be reduced by at least 2.07% compared with a single-mode benchmark strategy.

In the existing publications, different probability methods have been proposed in order to predict driver power demand by implementing Markov decisions. However, the prediction performance of each probability method is not yet evaluated considering the speed and acceleration characteristics of the driving cycles. The Markov chain state probability map is used to feature the speed and acceleration transition behavior of a driving cycle. However, each driving cycle has its own speed and acceleration characteristic. In other words, the Markov chain state probability maps can be different and even have big differences when the driving scenario is changed. Therefore, it is necessary to study the probability methods for power demand prediction applied in different driving scenarios. This paper implements a Markov chain based predictive energy management control method for a battery dual buffer system with a comparative study on two popular probability methods, namely maximum probability and weighted probability methods. The main contribution of this study is to reveal predictive performance of the above two probability methods by using different driving cycles. The research conclusions are expected to supply a basic reference for probability method selection when a Markov chain based predictive energy management strategy is designed.

2. ENERGY MANAGEMENT STRATEGY

In this paper, a Markov chain based predictive energy management strategy is proposed, as shown in Figure 2. In the strategy, a low-pass filter is employed for decomposing load power demand into low and high two frequency components, of which the low frequency power part is distributed to

the battery, and at the same time the high frequency power part is distributed to the supercapacitor. In this way, the frequency features of the fluctuating power demand can be effectively compensated by the supercapacitor. To reduce battery current and maintain the voltage level of supercapacitor, a fuzzy logic controller is developed. The input power demand of the fuzzy controller is estimated by a Markov chain model. Each part of the proposed energy management strategy will be explained detailedly in the following sections.

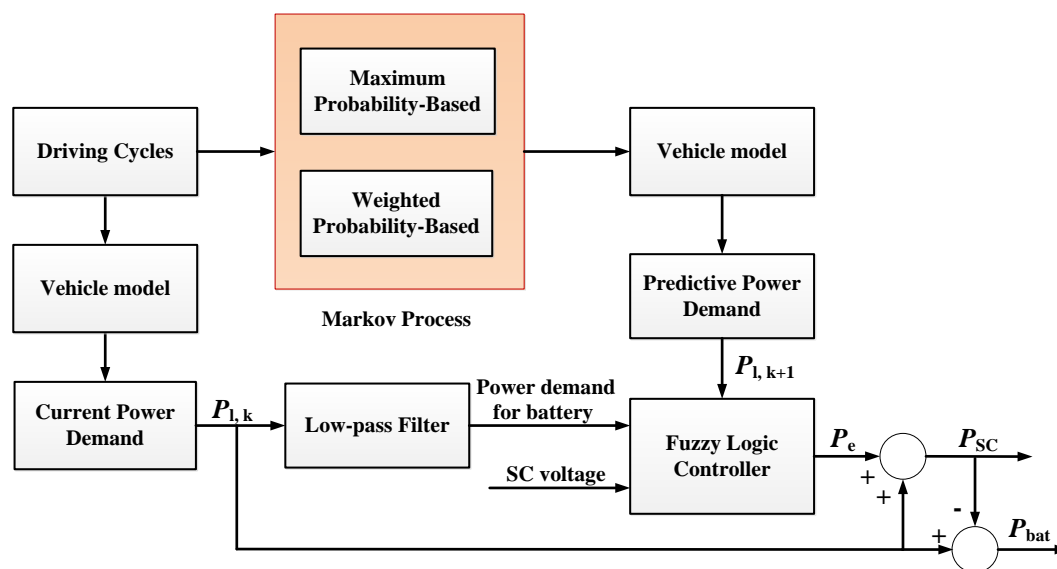


Figure 2. Implementation framework of the proposed predictive energy management strategy.

2.1. Frequency separation based on low-pass filter

In actual traffic condition, the power demand generated from the driver pedal operation is largely fluctuating. In the conventional single power system, the battery is often suffering from the largely fluctuating power demand, which would increase the internal resistance values of the battery and thus yield extensive power loss. To alleviate battery stress and improve work efficiency, a low-pass filter is employed to extract the low frequency component of the load power demand, denoted by PLF. Correspondingly, the supercapacitor power demand, denoted by PHF, is the difference between battery power demand and load power demand, denoted by Pload. Therefore, we have the following relationship expressions.

$$P_{LF} = F(P_{load}) \tag{1}$$

$$P_{HF} = P_{load} - P_{LF} \tag{2}$$

where F represents a low-pass filter function. This filter operation would stop battery from providing high frequency power demand and extend its lifetime.

2.2. Power demand prediction based on Markov chain model

In this work, we model vehicle acceleration state in the upcoming time step by the following first order Markov chain.

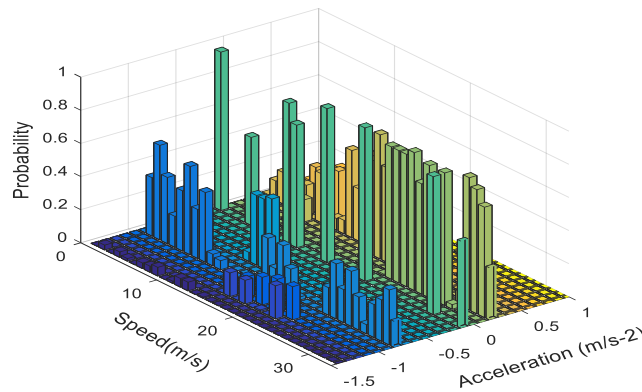
$$P_{ijm} = \Pr(a_{k+1} = i | a_k = j, v_k = s) \tag{3}$$

where vehicle speed v_k and acceleration a_k are Markov state parameters, P_{ijm} is the transition probability of vehicle acceleration, transferring from the acceleration state a_k at the current time step to the acceleration state a_{k+1} at the next time step while current vehicle speed $v_k = s$.

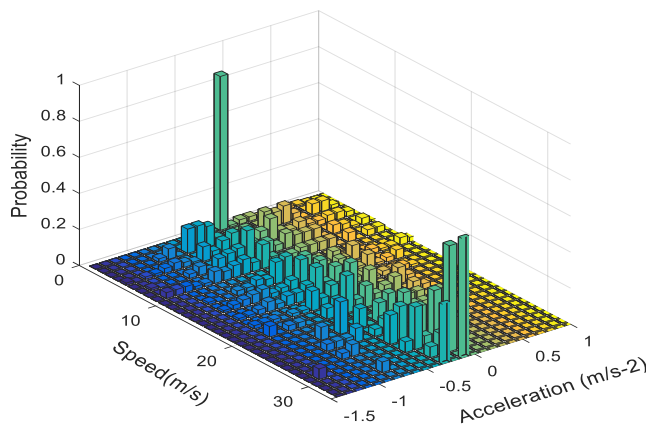
To obtain the Markov transition probabilities, the observation data need to be collected from selected driving cycles and then calculate by the following expression.

$$P_{i,j} = \frac{m_{i,j}}{m_i} \tag{4}$$

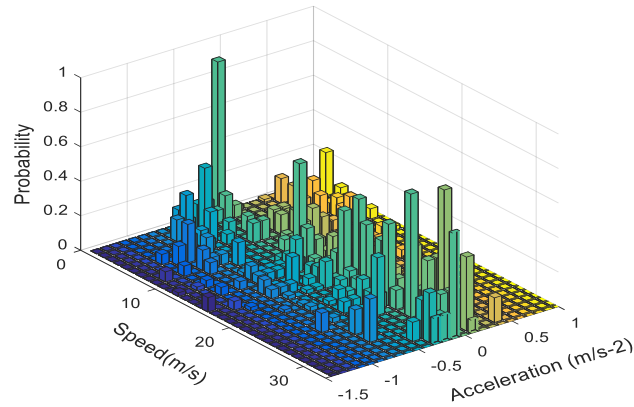
where $m_{i,j}$ represents the number of occurrences of vehicle acceleration state transition from a_k to a_{k+1} at vehicle speed $v_k = s$, m_i represents the total transition number of the acceleration a_k .



(a) Speed and acceleration characteristics of NEDC.



(b) Speed and acceleration characteristics of NurembergR36.



(c) Speed and acceleration characteristics of SC03.

Figure 3. Acceleration transition probabilities of NEDC, NurembergR36 and SC03 driving cycles.

Figure 3 shows the speed and acceleration characteristics of NEDC, NurembergR36 and SC03 driving cycles. It can be observed that the speed and acceleration characteristics of the three driving cycles are obviously different. Based on speed and acceleration information, the power demand at the next moment can be calculated in (5) and (6).

$$v_{k+1} = v_k + a_k \cdot t \tag{5}$$

$$P_{k+1} = \frac{v_{k+1}}{\eta} \left(mfg\cos(\theta) + mg\cos(\theta) + \frac{C_D A}{21.15} u_{k+1}^2 + \delta m a_{k+1} \right) \tag{6}$$

where the formula in (6) is a vehicle longitudinal dynamic model, which is used for power demand calculation. In the model, η represents energy deliver efficiency of the powertrain system, m represents vehicle weight, f represents rolling resistance coefficient of tires, g represents gravitational acceleration constant, A represents frontal area of vehicle, C_D represents drag coefficient, δ represents the conversion factor of rotational motion mass in a vehicle, θ represents road slope angle, here it is assumed to be zero, namely flat road surface. The parameter values of the vehicle model adopted in this study are given in Table 1.

Table 1. The parameter values of vehicle model adopted in this study.

Parameters	Values
m	1550
A	2.13
C_d	0.3
A	0.36
f	0.02
δ	1.1

In the vehicle model, the acceleration a_{k+1} at speed v_{k+1} condition would be estimated using maximum probability and weighted probability two methods, which can be respectively written by

$$a_{k+1} = \text{Maximum}(a_1, a_2, \dots, a_n) \quad (7)$$

$$a_{k+1} = a_1p_1 + a_2p_2 + \dots + a_np_n \quad (8)$$

2.3. Power distribution regulation based on fuzzy logic control

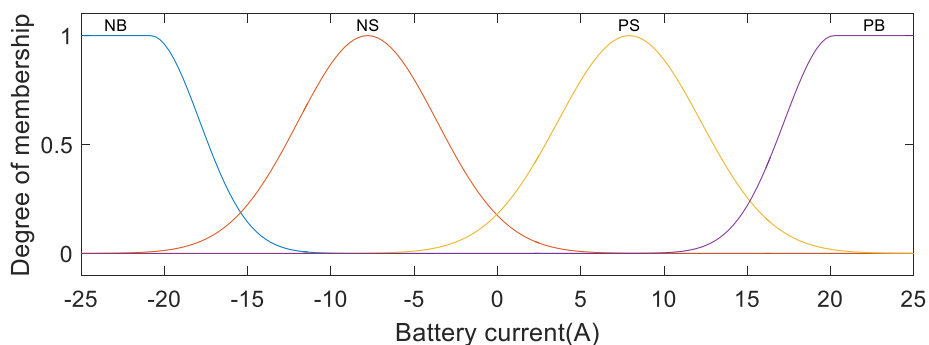
Although the power components obtained from the above frequency separation strategy can well match the frequency spectrum characteristics of the power sources, a supervisory control strategy is still necessary for reducing battery current and maintaining the voltage level of supercapacitor. From the energy management literature, the fuzzy logic controllers are widely used for managing power flow between the power sources due to their advantage in coping with uncertain and complicated systems. They make decisions depending on expert system rather than using a precise mathematical model of the system. Therefore, they can supply an appropriate control structure for the hybridized system with two different sources.

In this subsection, a fuzzy logic controller is developed for determining the appropriate power demand for battery and supercapacitor. The input parameters of the fuzzy controller are the low frequency current obtained from the low-pass filter and the voltage value of the supercapacitor, and the output parameter is the surplus current distributed to the supercapacitor for voltage regulation. Different types of membership functions are employed for partitioning the possible variation range of input and output parameters into several fuzzy areas. The current input parameter has four fuzzy domains, which are entitled with negative large (NL), negative small (NS), positive small (PS), positive large (PL). The supercapacitor voltage has three fuzzy domains, which are entitled with low (L), medium (M), high (H). The fuzzy domains used for the output parameter are similar with that of the current input parameter.

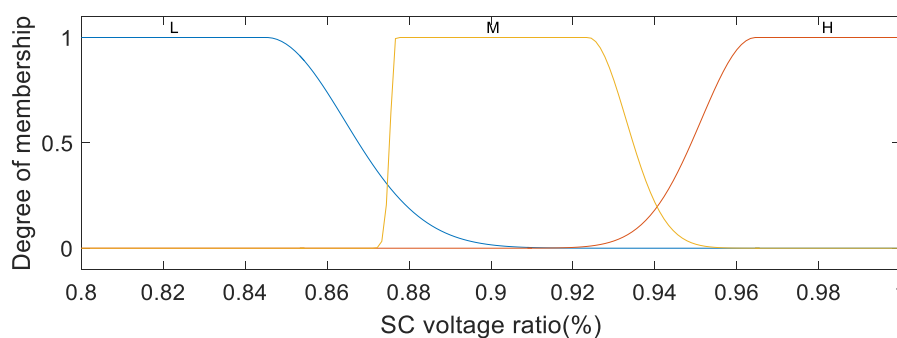
In order to obtain an improved fuzzy controller so that the battery current can be effectively reduced. The membership function curves of inputs and output are designed according to the possible power demand levels. For this, two specific cases are discussed as following.

(1) Case 1: an electric vehicle has the same driving state at current and next time interval, namely the electric vehicle is currently in driving state, according to Markov prediction, at the next time interval, it will be still in driving state; or the electric vehicle is currently in braking state, according to Markov prediction, at the next time interval, it will be still in braking state. Either driving or braking states, the fuzzy controller should can reasonably control the supercapacitor discharge for satisfying the continuous power supply of an electric vehicle. The fuzzy function relations between data import and export are plotted together using Figure 4. For the battery current, the Gaussian functions are utilized for dividing the current variations into four fuzzy areas from -25A to 25A, as pictured using Figure 4(a). In addition, the Gaussian function curves for current < -15 and current > 15 are modified with the trapezoidal function curves, where the battery current can be recognized more easily when it is becoming

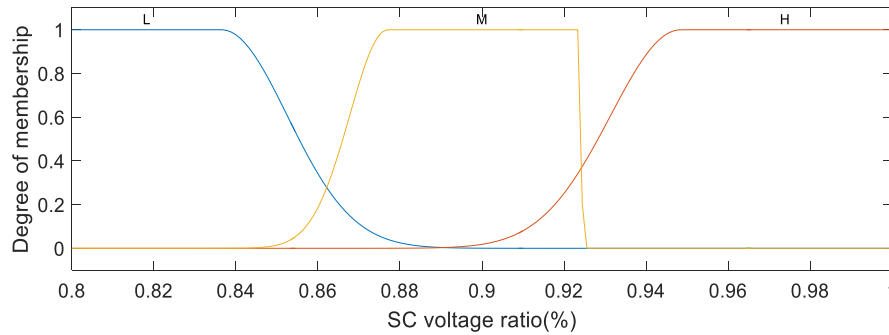
very large under driving or braking states. For the supercapacitor, in this work, the voltage variation is preset from 0.8 to 1.0. Two symmetric trapezoidal curves are employed for the low and high voltage areas, as shown using Figures 4(b) and (c). For the medium voltage range, the fuzzy membership is depicted using an asymmetry trapezoidal curve, which is finally determined by different simulation tests. The membership function curves of Figure 4(b) are used for the case that an electric vehicle has continuous driving demand at current and next time interval. It is clearly seen that the left curve of the asymmetry function is much cliffier, which indicates that the fuzzy logic controller will become more sensitive in controlling the supercapacitor discharge when the its voltage is low. Similarly, the membership function curves of Figure 4(c) are used for the case that an electric vehicle has continuous braking demand at current and next time interval. It is also seen that the right curve of the asymmetry function is much cliffier, which indicates that the fuzzy logic controller will become more sensitive in controlling the supercapacitor charge when the its voltage is high. For the surplus current, the layout of the membership function curves is the same with that of the battery current.



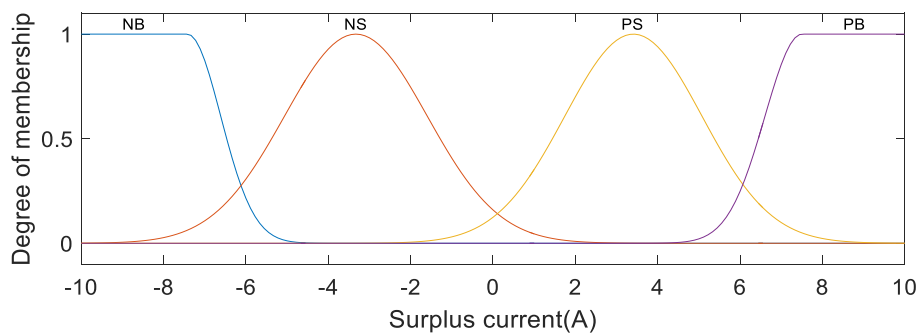
(a) The membership function curves of the import current.



(b) The fuzzy function relations of the supercapacitor voltage when a vehicle has continuous driving demand at current and next time interval.



(c) The fuzzy function relations of the supercapacitor voltage when a vehicle has continuous braking demand at current and next time interval.



(d) The fuzzy function relations of the export surplus current.

Figure 4. The fuzzy function relations of the import and export parameters.

(2) Case 2: an electric vehicle has inverse driving states at current and next time interval, namely the electric vehicle is currently in driving state, according to Markov prediction, at the next time interval, it may be in braking state; or the electric vehicle is currently in braking state, according to Markov prediction, at the next time interval, it may be in driving state. In this case, the membership function curves of battery current and surplus current are the same with that of the first case, but the membership function curves of the supercapacitor voltage need to be slightly adjusted as shown using Figure 5. The layout of the membership function curves is designed to be symmetric because the supercapacitor has completely different charge operations at current and next time interval. Table 2 displays the fuzzy rules that are utilized to combine surplus current to battery current and supercapacitor voltage.

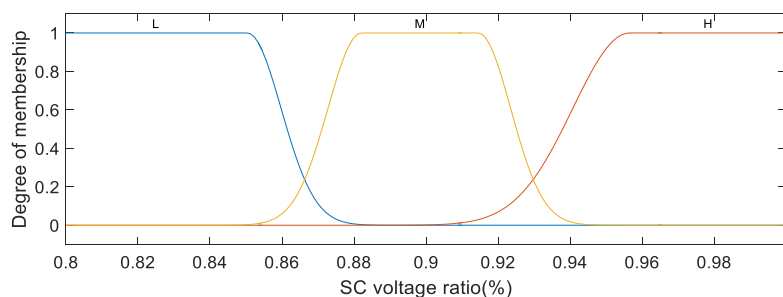


Figure 5. The membership function curves of the supercapacitor voltage when a vehicle has composite driving states at current and next time interval.

Table 2. Fuzzy rules for combining input and output variables.

dS	Ratio of supercapacitor voltage		
	L	M	H
NL	NL	NL	NS
NS	NL	NS	NS
PS	PS	PS	PL
PL	PS	PL	PL

3. EXPERIMENTAL CONFIGURATION OF HYBRID ENERGY STORAGE SYSTEM

In the subsection, a scaled-down hybrid energy storage system experimental configuration for a battery and supercapacitor has been established, as pictured using Figure 6. These experimental devices are composed of a 100V200A cycle simulator that is used to yield load current demand of an electric vehicle according to preset driving cycle, a Rapid prototyping controller from Huahai company in China that is used for implementing developed control algorithm between the energy sources, a bidirectional DC/DC converter that is used for regulating the voltage of the supercapacitor with a current supervision control.



Figure 6. The 72V hybrid system test bench, which consists of a battery pack as main source, a supercapacitor pack as aided source, a RapidECU for algorithm implement, a DC/DC converter for power flow regulation, a load simulator for cycle simulation, and a personal computer.

Table 3. Primary parameters and their ratings for DC/DC controller.

Names	Ratings
Peak voltage(V)	200
Peak current(A)	120
Rated power(kW)	20
Pack weight(kg)	15

For each implementing step of the implement control algorithm, the actual obtained supercapacitor power signal is compared with the desired power demand of the supercapacitor, which generated from the developed control model. The comparison result is then given to a designed PI controller and the output of the controller is the input of the DC/DC converter. The energy sources include a battery pack and a supercapacitor pack. The battery system is consisted of twenty-two cells by lithium iron phosphate material composition. The supercapacitor system is consisted of with six 48V Maxwell modules by iron oxide material composition. The main names of all the above several systems are given in Tables 3-6.

Table 4. Primary parameters and their ratings for load simulator.

Names	Ratings
Peak voltage (V)	100
Peak current (A)	200
Peak power (kW)	20

Table 5. Primary parameters and their ratings for battery pack.

Names	Ratings
Rated voltage(V)	72
Rated capacity(Ah)	50
Total cells	22
Peak power(kW)	3.6
Pack weight(kg)	50
Average resistance((mΩ)	80

Table 6. Primary parameters and their ratings for supercapacitor pack.

Names	Ratings
Rated voltage(V)	96
Rated capacity(F)	165
Module number	6
Peak power(kW)	9.6
Pack weight(kg)	45
Average resistance((mΩ)	2.9

4. RESULTS AND DISCUSSION

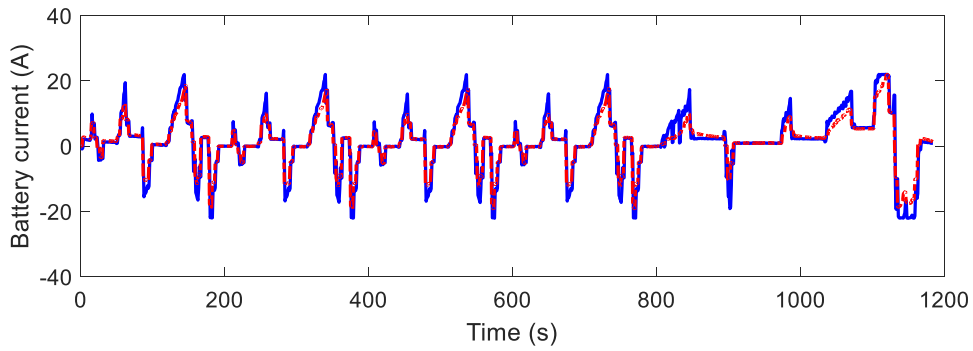
In this section, three different urban driving cycles, including NEDC, NurembergR36 and SC03, are chosen as test cycles. Considering the current and voltage limits of the actual battery and supercapacitor systems, the power demand of an electric vehicle using parameters displayed in Table 1 is scaled down by 5. Figures 7-9 give the experimental results of the proposed predictive energy management strategy using Markov chain with two different probability estimations. In the first method, the future power demand is

predicted using Markov chain with maximum probability estimation, and in the second method, the future power demand is predicted using Markov chain with weighted probability estimation[36,41,42].

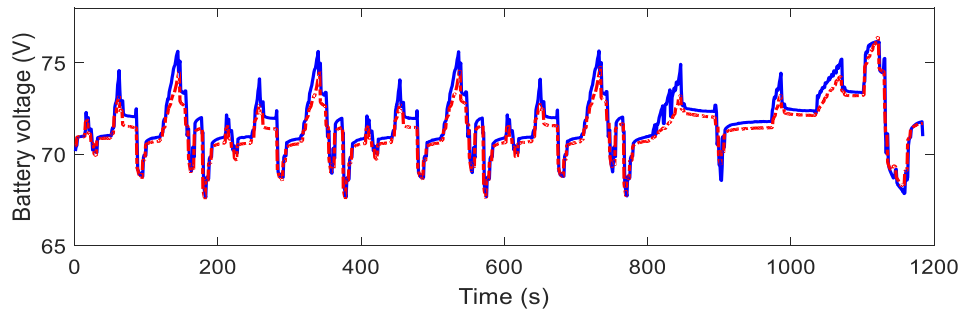
The dynamic behaviors of battery current under NEDC driving cycle are compared in Figure 7(a). The red indicates the results that are obtained using Markov chain with maximum probability estimation, and the blue indicates the results that are obtained using Markov chain with weighted probability estimation. From the curves, we can find that the battery current by maximum probability estimation is obviously smaller than that by weighted probability estimation. However, from the results of Figure 8(a) and Figure 9(a) under NurembergR36 and SC03 driving cycles respectively, we have inverse observation, that the battery currents by maximum probability estimation are relatively larger than that by weighted probability estimation. This indicates that the prediction accuracy of Markov probability estimation methods is dependent on the transition behaviors of the state variables in a driving cycle.

Figures 7-9(b) give the experimental comparative results of battery voltage under NEDC, NurembergR36 and SC03 driving cycles. We can observe that the control strategy with both probability estimation methods can realize a good voltage stability. For the NEDC driving cycle, the maximum voltage drop is 8.88V by maximum probability estimation, which is a bit larger than 8.55V by weighted probability estimation. Still, at most time of the driving cycle, the voltage drops by maximum probability estimation is much smaller than that by weighted probability estimation. From the voltage results of NurembergR36 and SC03 driving cycles, at most time of the driving cycle, the voltage drops by maximum probability estimation is much larger than that by weighted probability estimation. These observations prove that the Markov chain with maximum probability estimation can realize higher predictive precision for NEDC driving cycle, and the Markov chain with weighted probability estimation can realize higher predictive precision for NurembergR36 and SC03 driving cycles.

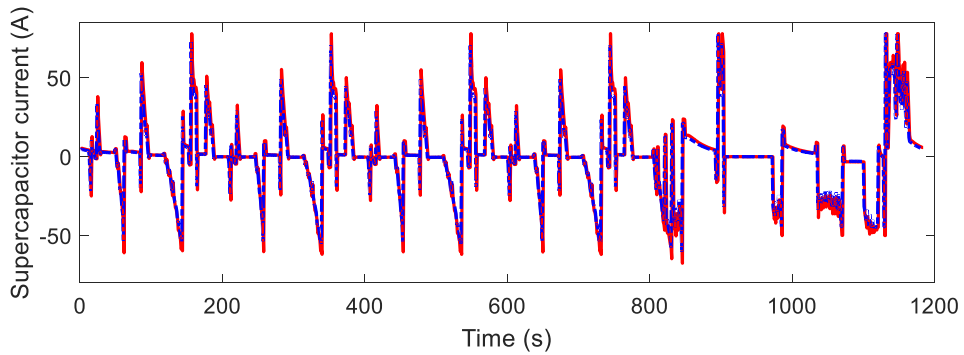
The curve evolutions of supercapacitor current under NEDC, NurembergR36 and SC03 driving cycles are illustrated in Figures 7-9(c). Since the current demands generated from the three driving cycles are provided by the battery and supercapacitor jointly, therefore, if the battery current is large, then the supercapacitor current should be small based on fixed current demand, and vice versa. From Figure 9(c), the control strategy with maximum probability estimation can control the supercapacitor to provide larger charge-discharge current compared with that with weighted probability estimation under NEDC driving cycle. This can prevent the battery from large current shock and extend its lifetime. In addition, owing to low resistance and high energy delivery efficiency, more regenerative braking energy can be effectively recovered by the supercapacitor. Figure 7(d) illustrates the experimental comparative results of supercapacitor voltage under NEDC driving cycle. We can find that the lowest voltage point of the supercapacitor is above 75V, namely the voltage doesn't exceed its lower limitation (in this study, the lower limitation of the supercapacitor voltage is set to be 75V). The conclusions for the supercapacitor current comparison under NurembergR36 and SC03 driving cycles are the same, namely the control strategy with weighted probability estimation can control the supercapacitor to provide larger charge-discharge current compared with that with maximum probability estimation. It should be noted from Figure 8(d) and Figure 9(d), that the lowest points of the supercapacitor voltage are all above 80V. This can be explained that smaller power demands are requested for NurembergR36 and SC03 driving cycles.



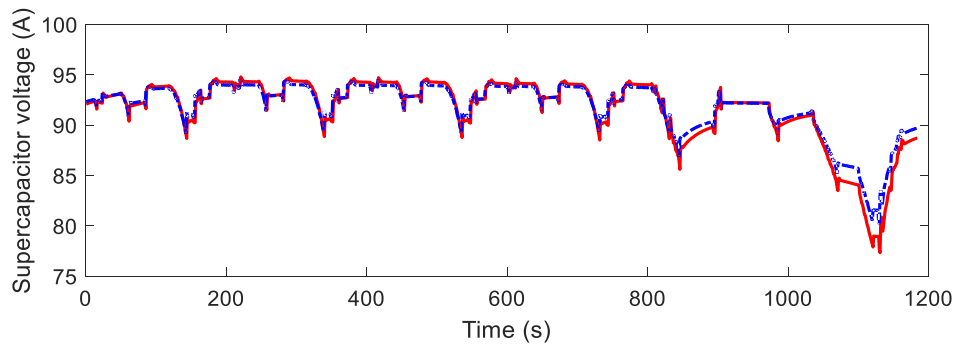
(a) Experimental comparative results of battery current.



(b) Experimental comparative results of battery voltage.

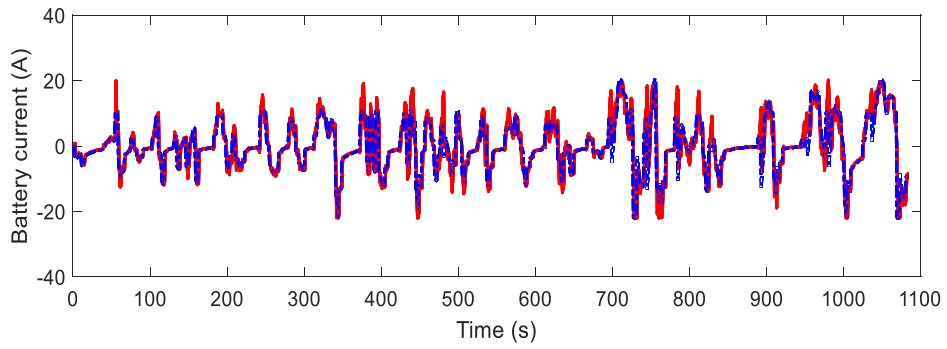


(c) Experimental comparative results of supercapacitor current.

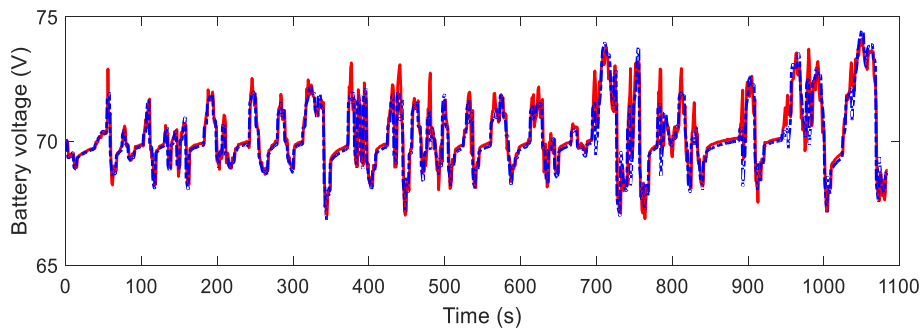


(d) Experimental comparative results of supercapacitor voltage.

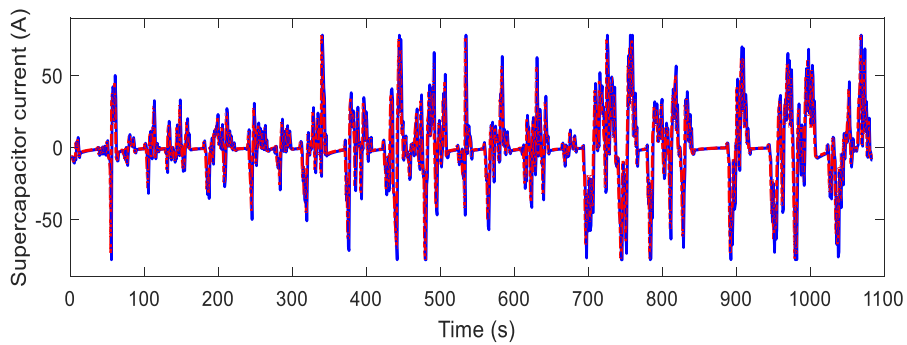
Figure 7. Voltage and current behaviors of battery and supercapacitor under NEDC driving cycle. The red indicates the results that are obtained using maximum probability method, and the blue indicates the results that are obtained using weighted probability method.



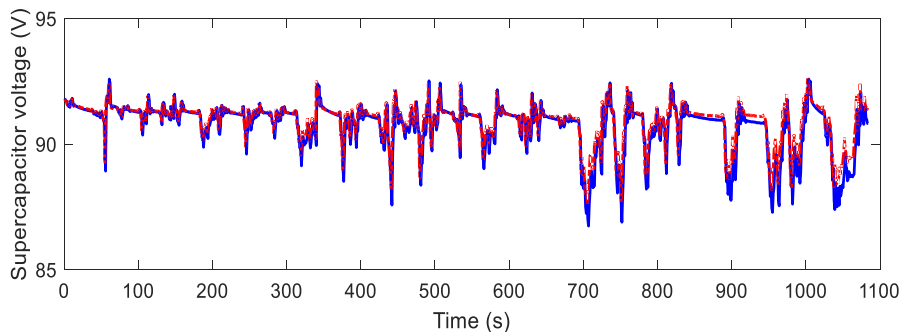
(a) Experimental comparative results of battery current.



(b) Experimental comparative results of battery voltage.

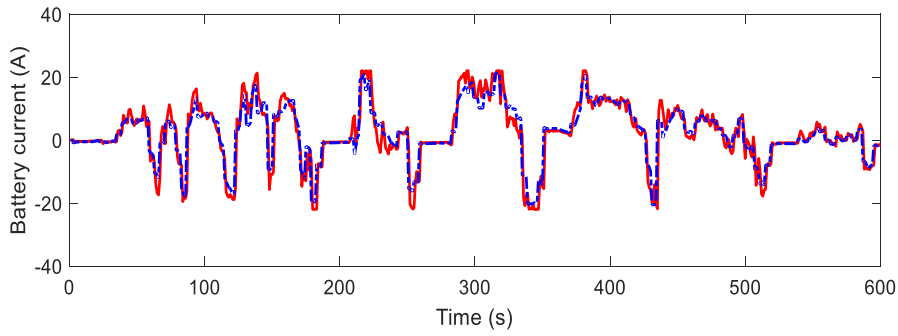


(c) Experimental comparative results of supercapacitor current.

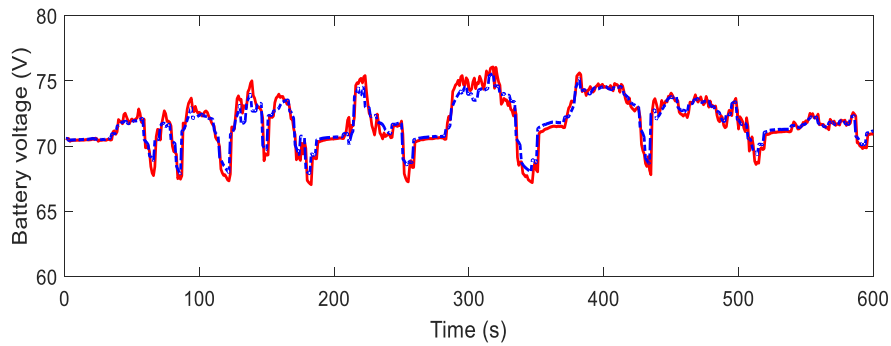


(d) Experimental comparative results of supercapacitor voltage.

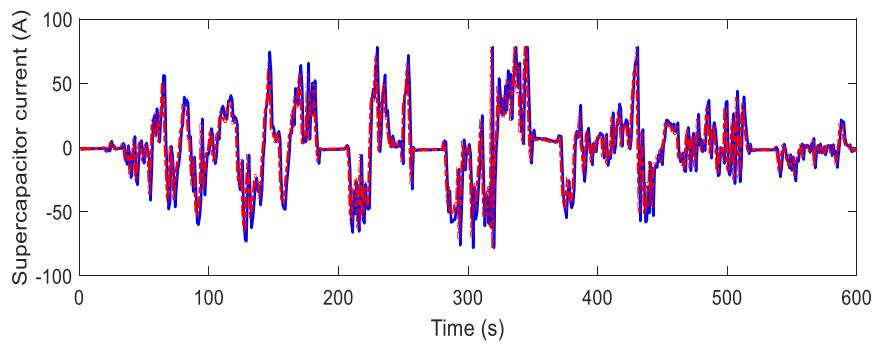
Figure 8. Voltage and current behaviors of battery and supercapacitor under NurembergR36 driving cycle. The red indicates the results that are obtained using maximum probability method, and the blue indicates the results that are obtained using weighted probability method.



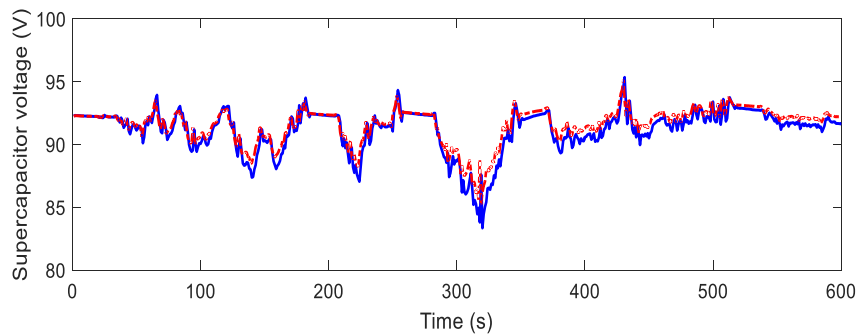
(a) Experimental comparative results of battery current.



(b) Experimental comparative results of battery voltage.



(c) Experimental comparative results of supercapacitor current.



(d) Experimental comparative results of supercapacitor voltage.

Figure 9. Voltage and current behaviors of battery and supercapacitor under SC03 driving cycle. The red indicates the results that are obtained using maximum probability method, and the blue indicates the results that are obtained using weighted probability method.

5. CONCLUSIONS

This paper introduced a predictive energy management strategy and its experiment implementation for battery and supercapacitor hybrid energy storage systems of electric vehicles. In the strategy, a low-pass filter was designed for removing the high-frequency component of the battery power demand. A fuzzy logic controller was developed using future power demand information of a driving cycle for enhancing the performance in shaving battery peak current and maintaining the voltage level of supercapacitor. The future power demand information was obtained from a Markov chain model using two probability estimation methods for the purpose of comparison, namely maximum probability estimation and weighted probability estimation. A scaled down battery and supercapacitor hybrid system experimental test platform was developed to implement energy management strategy based on NEDC, NurembergR36 and SC03 Driving cycles. Experimental results showed that the proposed strategy could achieve expected control performance. Here two findings are summarized. One is that the battery peak current was obviously reduced and at the same time the high-frequency component was effectively avoided, which can eventually increase the lifetime of the battery. Another is that the strategy with maximum probability estimation performs better if the state transition probabilities of Markov chain are obtained from NEDC driving cycle, whereas the strategy with weighted probability estimation performs better if the state transition probabilities of Markov chain are obtained from NurembergR36 and SC03 driving cycles.

ACKNOWLEDGMENTS

This work was supported in part by Project of Liaoning Province Major Technology Platform grant JP2017002, Guidance Plan of Natural Science Foundation of Liaoning Province grant 20180551280, National Science Foundation of China grant 51675257, Project of Liaoning Province Innovative Talents grant LR2016054, overseas Training Program for colleges and universities of Liaoning Province grant 2018LNGXGJWPY-YB014 and the development grants from Shenzhen Science, Technology and Innovation Commission (JSGG20170822145318071).

References

1. C. M. Martinez, X. Hu, D. Cao, E. Velenis, B. Gao, and M. Wellers, " *IEEE Trans. Vehicular Technology*, 66(2017) 4534.
2. S. Manzetti and F. Mariasiu, *Renew. Sustain. Energy Reviews*, 51(2015) 1004.
3. A. M. Andwari, A. Pesiridis, S. Rajoo, M.B. Ricardo and V. Esfahanian, *Renew. Sustain. Energy Reviews*, 78(2017) 414.
4. M. Hannan, F. Azidin and A. Mohamed, *Renew. Sustain. Energy Reviews*, 29(2014) 135.
5. M. Hannan, M. Hoque, A. Mohamed and A. Ayob, *Renew. Sustain. Energy Reviews*, 69(2017) 771.
6. L. Kouchachvili, W. Yaïci and E. Entchev, *J. Power Sources*, 374(2018) 237.
7. J. Shen, S. Dusmez and A. Khaligh, *IEEE Trans. Ind. Informat.*, 10(2014), 2112.
8. S. F. Tie and C. W. Tan, *Renew. and Sustain. Energy Reviews*, 20(2013) 82.
9. C. Holland, J. Weidner, R. Dougal and R. White, *J. Power Sources*, 109(2002) 32.
10. N. Omar, M. Daowd, O. Hegazy, P. Bossche, T. Coosemans and J. Mierlo, *Energies*, 5(2012) 4533.
11. A. Kuperman and I. Aharon, *Renew. Sustain. Energy Reviews*, 15(2011)981.
12. L. Lam and R. Louey, *J. Power Sources*, 158(2006)1140.
13. P. Bentley, D.A. Stone and N. Schofield, *J. Power Sources*, 147(2005)288.

14. M. E. Choi, S. W. Kim and S.-W. Seo, *IEEE Trans. Smart Grid*, 3(2012) 463.
15. A. Burke and M. Miller, *J. Power Sources*, 196(2011) 514.
16. Z. Song, J. Li, X. Han, L. Xu, L. Lu, M. Ouyang and H. Hofmann, *Appl. Energy*, 135(2014) 212.
17. S. Pay and Y. Baghzouz, *Proc. IEEE Power Tech Conf.*, Bologna, Italy, 2003, 1-6.
18. K. Chau and Y. Wong, *Energy Convers. Management*, 42(2001) 1059.
19. C. Xiang, Y. Wang, S. Hu and W. Wang, *Energies*, 7(2014) 2874.
20. S. G. Wirasingha and A. Emadi, *IEEE Trans. Vehicular Technology*, 60(2011) 111.
21. L. Kouchachvili, W. Yaïci, E. Entchev, *J. Power Sources*, 374(2018) 237.
22. L. Xu, M. Ouyang, J. Li and F. Yang, *Proc. IEEE ISIE*, Hangzhou, China, 2012, 1490–1495.
23. O. Hegazy and J. V. Mierlo, *Int. J. Veh. Des.*, 58(2012)200.
24. J. P. Ribau, C. M. Silva and J. M. C. Sousa, *Appl. Energy*, 129(2014)320.
25. C. Li and G. Liu, *J. Power Sources*, 192(2009)525.
26. C. Yang, S. Du, L. Li, S. You, Y. Yang, Y. Zhao, *Appl. Energy*, 203(2017)883.
27. B. Hredzak, G. V. Agelidis and M. Jang, *IEEE Trans. Power Electron.*, 29(2014) 1469.
28. J. P. Trovão, P. G. Pereirinha, H. M. Jorge and C. H. Antunes, *Appl. Energy*, 105(2013)304.
29. B. Wang, J. Xu, B. Cao and X. Zhou, *J. Power Sources*, 281(2015)432.
30. J. Armenta, C. Núñez, N. Visairo and I. Lazaro, *J. Power Sources*, 284(2015) 452.
31. A. Ferreira, J. Pomilio, G. Spiazzi and L. A. Silva, *IEEE Trans. Power Electron.*, 23(2008) 107.
32. Q. Zhang, G. Li , *IEEE Trans. Power Electron.*, 35(2020) 1014.
33. Y. He, W. Zhou, M. Li, C. Ma and C. Zhao, *IEEE Trans. Transportation Electrification.*, 2(2016) 300.
34. X. Zhang, C. C. Mi, A. Masrur, D. Daniszewski, *J. Power Sources*, 185(2015)1533.
35. M. Michalczuk, B. Ufnalski and L. M. Grzesiak, *International Journal for Computation and Mathematics in Electrical and Electronic Engineering*, 34(2008) 173.
36. Y. Wang, W. Wang, Y. Zhao, L. Yang and W. Chen, *Energies* 9(2016) 1.
37. B. Asadi and A. Vahidi, *IEEE Trans. Contr. Syst. Technol.*, 19(2011)11.
38. C. Zhang, A. Vahidi, P. Pisu, X. Li, K. Tennaut, *IEEE Trans. Veh. Technol.*, 3(2010)1139.
39. R. Langari, J.S. Won, *IEEE Trans. Veh. Technol.*, 3(2005)925.
40. K. Song, F. Li, X. Hu, L. He, W. Niu, S. Lu, T. Zhang, *J. Power Sources*, 389(2018)230.
41. H. Hemi, J. Ghouili, A. Cheriti, *Energy Conver. and Manage.*, 91(2015) 387.
42. Yang Zhou, Alexandre Ravey, Marie-Cecile Péra, *Appl. Energy*, 258(2020) 1140.